Journal of Applied Polymer Science

# The morphology and gas-separation performance of membranes comprising multiwalled carbon nanotubes/polysulfone–Kapton

**Seyed Farzad Soleymanipour,[1] Amir Hossein Saeedi Dehaghani,[2] Vahid Pirouzfar,[3] Afahar Alihosseini[4]**

[1]Department of Chemical Engineering, Shahreza Branch, Islamic Azad University, Shahreza, Iran
[2]Petroleum Engineering Group, Faculty of Chemical Engineering, Tarbiat Modares University, P.O. Box 14115-114, Tehran, Iran
[3]Young Researchers and Elite Club, Central Tehran Branch, Islamic Azad University, Tehran, Iran
[4]Department of Chemical Engineering, Islamic Azad University, Central Tehran Branch, Tehran, Iran
Correspondence to: A. H. Saeedi Dehaghani (E-mail: asaeedi@modares.ac.ir)

**ABSTRACT:** The development of desirable chemical structures and properties in nanocomposite membranes involve steps that need to be carefully designed and controlled. This study investigates the effect of adding multiwalled nanotubes (MWNT) on a Kapton–polysulfone composite membrane on the separation of various gas pairs. Data from Fourier transform infrared spectroscopy and scanning electron microscopy confirm that some studies on the Kapton–polysulfone blends are miscible on the molecular level. In fact, the results indicate that the chemical structure of the blend components, the Kapton–polysulfone blend compositions, and the carbon nanotubes play important roles in the transport properties of the resulting membranes. The results of gas permeability tests for the synthesized membranes specify that using a higher percentage of polysulfone (PSF) in blends resulted in membranes with higher ideal selectivity and permeability. Although the addition of nanotubes can increase the permeability of gases, it decreases gas pair selectivity. Furthermore, these outcomes suggest that Kapton–PSF membranes with higher PSF are special candidates for $CO_2/CH_4$ separation compared to $CO_2/N_2$ and $O_2/N_2$ separation. High $CH_4$, $CO_2$, $N_2$, and $O_2$ permeabilities of 0.35, 6.2, 0.34, and 1.15 bar, respectively, are obtained for the developed Kapton–PSF membranes (25/75%) with the highest percentage of carbon nanotubes (8%), whose values are the highest among all the resultant membranes. © 2016 Wiley Periodicals, Inc. J. Appl. Polym. Sci. **2016**, *133*, 43839.

**KEYWORDS:** graphene and fullerenes; membranes; nanotubes; oil & gas; polyimides; separation techniques

Received 4 January 2016; accepted 26 April 2016
**DOI: 10.1002/app.43839**

## INTRODUCTION

Within the last few decades, energy consumption industries have been widely developed.[1,2] The $CO_2/N_2$, $CO_2/CH_4$, $O_2/N_2$, and $N_2/CH_4$ purification processes are used to separate gases in the conservation and recovery of energy, refinery, chemical processing, and fertilizer industries.[3–6] Currently, commercially available purification and recovery techniques for this approach are gas sweetening, swing adsorption, amine treating, and cryogenic procedures, which have high costs and high energy use.[7–10] Within the last few years, researchers have been greatly interested in synthesizing novel membranes for gas-separation systems. High efficiency and productivity and low consumption of energy are regarded as the most important objectives in designing such systems.[11,12] The trade-off between efficiency (selectivity) and productivity (permeability) is considered to be a significant limitation in membrane processes.[13] Accordingly, membranes used for gas separation are compared with an upper bound correlation by Robeson.[13,14] Polymer membranes have not shown high gas separation performance because of their low productivity and efficiency and limitation by an upper bound. New membranes and procedures of membrane fabrication are being scrutinized to improve the separation performance of membranes (especially polymer membranes). Among the various high-performance gas-separation membranes, composite and mixed-matrix membranes are well above Robeson's upper bound trade-off curve.[15–21] These novel and modified membranes started to emerge as an alternative approach in separation technology and membrane science in order to overcome the production and process limitations. They have been produced from suitable polymers and fillers.[22–25] Mainly nonorganic materials are used in the synthesis of composite membranes. Studies on nanotubes to fabricate composite membranes demonstrate that these substances are identified as the most suitable material for the transportation of light gases such as methane and hydrogen in comparison to other substances with the same pore sizes.[26–30] The optimized size distribution of

these nanotubes leads to composite membranes with high quality and efficiency in comparison to polymeric membranes.[31,32] The production of these composite materials contributes to achieving a better membrane with more acceptable specifications and transport properties than both types of polymeric and inorganic membranes, such as permeability and selectivity and suitable mechanical and thermal resistance.[32,33]

Within the last decade, polymeric membranes with good chemical and thermal stability and high selectivity and gas flux, along with inorganic particles (e.g., zeolite,[34] carbon molecular sieves[35–38], inorganic oxides,[39] and organic fillers[40] (e.g., fullerenes and carbon nanotubes (CNT)[41–49], have been applied in the preparation of composite membranes. Various combinations of fillers and polymers result in diverse interface morphologies, which lead to special influences on gas-separation performance. This is because the synthesis of composite membranes generally involves difficulties like poor size distribution of the dispersed phase and weak particle contact in the matrix of the polymer.

Engineering polymers of polysulfone (PSF) groups,[50–52] polycarbonates,[53] poly(aryl ketones), and polyimides (PI)[54–59] have demonstrated specifications like the applied material in the composite membranes. Among the polymeric precursors in the preparation of composite membranes, polysulfones and polyimides are the most fascinating because of their excellent properties, such as high productivity and efficiency of separation, high thermal and chemical stability, high mechanical resistance, and ease of preparation.[8,60–64] They tend to have the highest gas transport properties of the polymer families, but even the best solution polymeric membranes are limited by an upper bound of possible gas selectivity and permeability. The high gas selectivity, combined with a relatively high gas permeability, allows many of these membranes to operate above the upper bound.[64]

Ansaloni *et al.*[58] put into practice different functionalities in multiwalled nanotubes with a diameter of 10–15 nm and synthesized poly(vinyl acetate) (PVA)/multiwalled nanotube (MWNT) membranes displaying high $CO_2$ permeability and good gas pair selectivity for $CH_4$, $H_2$, and $N_2$. In addition, Zhao *et al.*[59] applied amino-modified multiwalled carbon nanotubes to prepare mixed-matrix membranes (MMMs). The results showed that the normalized $N_2$, $CH_4$, and $CO_2$ permeability had almost the same increase and the $CO_2/N_2$, $CO_2/H_2$, and $CO_2/CH_4$ selectivity remained constant with increasing MWNT–$NH_2$ content. Thus, the incorporation of MWNT–$NH_2$ significantly enhanced the gas permeation properties of polymer/MWNT–$NH_2$ MMMs.

In the present work, the gas properties of the composite membranes are evaluated. The main objectives of this research are to explore the effect of the polymer precursor blended molecular structures and of the percentage of multiwalled carbon nanotubes in a polymeric matrix to provide a direction for investigators in the field of fabrication and design of high-performance membranes. Two engineering polymers (Kapton and PSF) with different chemical structures were chosen for this comprehensive study. The applicable procedures for fabricating new membranes with good performance are analyzed. To the best of our knowledge, this is the first study on the preparation of composite membranes derived from polymeric blend precursors comprising PSF, Kapton, and MWNT. The composite membranes fabricated in this investigation can be developed as applicable membranes with extremely good performance in gas-separation efficiency and transport productivity for the main gases (such as $O_2$, $N_2$, $CO_2$, and $CH_4$) in industrial applications.

## EXPERIMENTAL

### Materials

The materials used in this research work were Kapton poly (pyromellitic dianhydride-*co*-4,4′-oxydianiline; PMDA-ppODA), which was purchased from DuPont, Boston, MA, USA. and polysulfone, which was prepared by the Aldrich Chemical Company Inc. (Milwaukee, USA). Carbon nanotubes with high purity (middle diameter: 10–15 nm, length: 5–15 mm, 116 $m^2/g$) as nonorganic fillers were supplied by TECNAN (Tecnologia. Navarra de Nanoproductos S.L, Spain). Other chemicals such as dimethylacetamide 98% (DMAC) as solvent, sulfuric acid 98%, and nitric acid 65% were purchased from Merck (Darmstadt, Germany) and used without purification. The $N_2$, $CH_4$, $CO_2$, and $O_2$ gases used had 99.99% purity.

### Functionalization Method for MWNTs and Synthesis of Composite Membranes

Nitric acid and sulfuric acid with a volume ratio of 1:3 was used to oxidize the carbon nanotubes. The oxidation of nanotubes with oxidizing acid produced numerous functional groups, such as hydroxyl (OH), carboxyl (COOH), and carbonyl (C═O), on the surface of the nanotubes. These functional groups connected on the surface of the nanotubes, causing an increase in the specific surface area of the nanotubes.

A mixed membrane consisting of Kapton–PSF (50/50 wt %) with multilayer carbon nanotubes was synthesized with the dry/wet phase inversion method. Before preparing the solution, the polymer powder and carbon nanotube particles were put in an oven at 80 °C for a few hours in order to dry them and eliminate the humidity. Kapton–PSF (50/50 wt %) was dissolved in DMAC at 10 wt % at 70 °C to produce a homogenous mixture. The final solution was cast in a glass and held for a period of 12 h at 65 °C in an oven. The prepared membrane was placed in a vacuum oven at 75 °C for a period of 8 h to complete the process of solvent removal. To synthesize the nanocomposite membrane, first, the carbon nanotube particles were dispersed with different polymer weight percentages of 2.5, 5, and 8, for a period of 3 h, then the considered polymer was added to the homogenous solution and stirred for a period of 3 h to produce a homogenous and steady solution. This solution was used for membrane casting. The thickness of the pure and developed nanocomposite membranes was about 50 micron.

### Characterization

Functional structures and groups of nanocomposite membranes were studied with a Fourier transform infrared spectrometer (FTIR PerkinElmer, Shelton, USA) BIO-RAD FTS-7 in the range of 400–4000 $cm^{-1}$. A scanning electron microscope (SEM) (Philips, The Netherlands) KYKY-EM 3200 was used to study the morphology and manner of the nanoparticle distribution in the modified membranes. Subsequently, the thermal properties

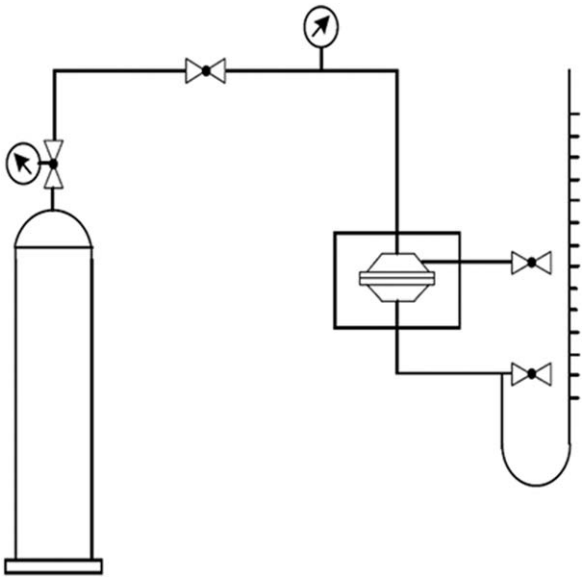

**Figure 1.** Schematic of the applied separation test setup.

of the membranes were determined by differential scanning calorimetry (DSC) (Mettler, Switzerland) using a Rheometric Scientific STA1500 with Ar purging at a flow rate of 30 mL $min^{-1}$.

### Gas Permeability Test

The permeability and ideal selectivity of the membranes are determined for the pure gases $N_2$, $O_2$, $CO_2$, and $CH_4$ at 30 °C and 10 bar. A schematic of the applied separation test setup is presented in Figure 1. The flow rate of gas transportation was assessed by a bubble flow meter, and each test was repeated at least two times. Equation (1) is used to calculate the gas permeability:

$$P = \frac{ql}{(P_1 - P_2)A} \tag{1}$$

The gas permeability was calculated from the rate of pressure increase at steady state using the following equation:

$$P = \frac{273.15 \times 10^{10} vl}{760AT[(p_0 \times 76)/14.7]} \left(\frac{dp}{dt}\right) \tag{2}$$

where $P$ is the gas permeability of the membrane in units of Barrer (1 Barrer = $1 \times 10^{-10}$ $cm^3$ (STP) cm $cm^{-2}$ $s^{-1}$ $cmHg^{-1}$), $v$ is the volume of the downstream chamber ($cm^3$), $A$ is the effective area of the membrane ($cm^2$) (this is the same in the permeability test for all the membranes), $l$ is the membrane thickness (cm), $T$ is the operating temperature (K), and the feed gas pressure in the upstream is given by $P_0$ in psia. The ideal separation factor (selectivity) is defined as the ratio of permeabilities of a pure gas pair:

$$\alpha_{A/B} = \frac{P_A}{P_B} \tag{3}$$

## RESULTS AND DISCUSSION

### Polymer Structure by FTIR

The molecular structures of the composite membrane and the carbon nanotubes have been studied by FTIR. This test is conducted to confirm the reliability of both the functionalization of the carbon nanotubes and the existence of particles in the structure of the composite membranes. Furthermore, it is essential to scrutinize the interaction between the particles and polymer matrix in the network. The FTIR spectra of pure and functionalized carbon nanotubes are presented in Figure 2. In comparing the two infrared spectra of the preliminary and functionalized nanotubes, the existence of new functional groups can be clearly observed because of a new absorption peak in the spectrum. A small wide peak at 3070 $cm^{-1}$ is also observed and may be related to C—H tensional absorption. An absorption peak at 2419 $cm^{-1}$ is observed in the functionalized nanotube spectrum arising from the absorption band of the O—H group. The peak related to the C═O imide group is present at 1722 $cm^{-1}$.

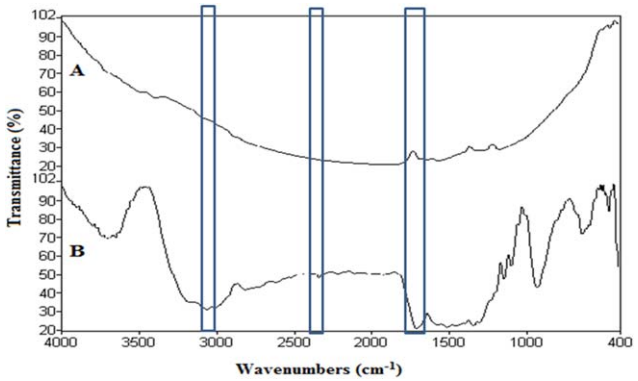


**Figure 2.** FTIR spectrum of (A) pure carbon nanotube, (B) functionalized carbon nanotube. [Color figure can be viewed in the online issue, which is available at wileyonlinelibrary.com.]

The FTIR spectra of nanocomposite membranes composed of Kapton–PSF/carbon nanotubes are shown in Figure 3. These figures feature the peaks related to C—H stretching vibrations at 2923 $cm^{-1}$ and the peaks related to C═C double-bond vibrations at 1677 $cm^{-1}$. In addition, the range 726 to 1383 $cm^{-1}$ indicates the existence of heterocyclic rings. Adding carbon nanotubes will display the existence of functional groups in carbon nanotube. The main absorption bands are 1050 $cm^{-1}$, which is related to the $SO_2$ groups in PSF; 2700 $cm^{-1}$, for the $CH_3$ groups in PSF; 3200 $cm^{-1}$, for the aromatic rings in PSF; and 1700 $cm^{-1}$, for the $NH_2$ groups in amino CNTs.

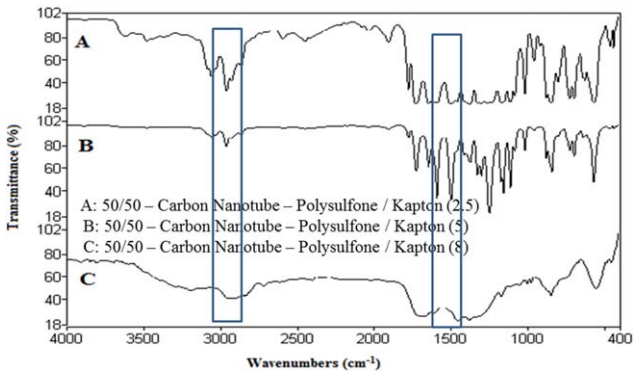


**Figure 3.** Comparison between FTIR spectra of nanocomposite membranes (50/50) with different percentages of carbon nanotubes. [Color figure can be viewed in the online issue, which is available at wileyonlinelibrary.com.]

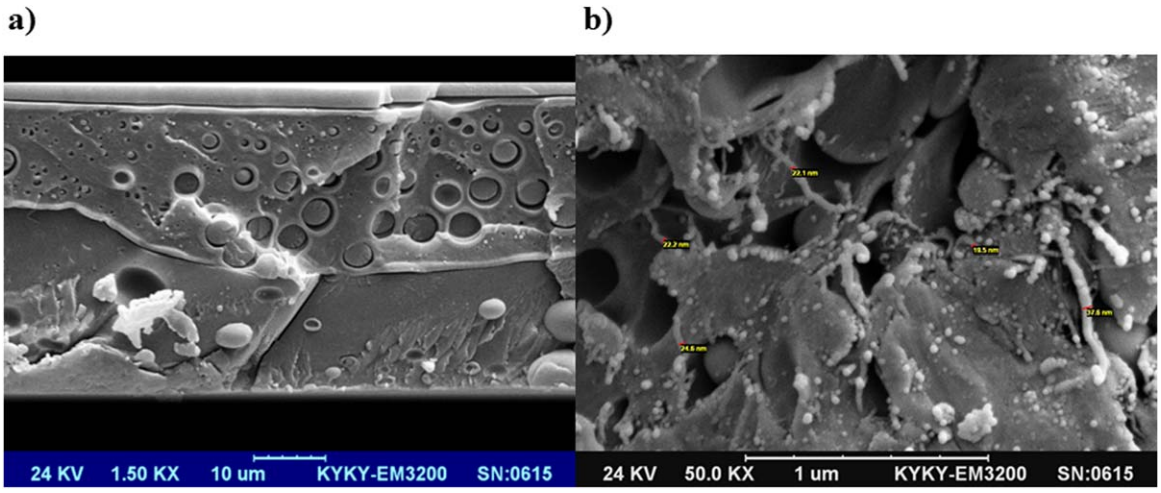


**Figure 4.** Scanning electron microphotographs of (a) synthetic membranes with PSF percentages of 50% of Kapton and PSF and (b) nanocomposite membranes with PSF percentages of 50% in Kapton–PSF and 2.5% of multilayer carbon nanotubes. [Color figure can be viewed in the online issue, which is available at wileyonlinelibrary.com.]

### Polymer Structure and Characteristics

Figures 4 and 5 illustrate the scanning electron microphotographs of width-wise sections of PI–PSF synthetic membranes and nanocomposites with different percentages of carbon nanotubes. These figures show a spherical distribution of a phase in another phase. However, they show the structure of the formation of a layer of polymer. Such a phenomenon occurs because of the unsuitable adaptation of two polymers with one another, and finally this causes a phase separation in the structure. A study of the preparation of the nanocomposite shows that the carbon nanotubes have a tendency to exist as a continuous phase. Holistically, it is observed that nanotubes have a homogenous distribution in the polymer network, and there is no defect on the membrane and no emergence of two phases of polymer/nanotubes. Conclusively, there is an appropriate adaptation between the two phases of polymer and nanotubes. The cross-sectional figures reveal that there are some fibers with diameters of 29 to 40 nm. Given that the diameter of nanotubes has been reported in the range of 15–18 nm, this implies that a thin layer of polymer has coated the surface. This phenomenon confirms the effective improvement of the surface, which promotes a suitable interaction of the nanotube surface with the polymer. In the presence of the carbon nanotube (Figures 4 and 5), no agglomeration is observed. This means that nanotubes have been distributed through the matrix very well.

### Gas Property Results

Table I presents the permeability and ideal selectivity of oxygen, nitrogen, carbon dioxide, and methane gases versus carbon nanotube percentage in conditions of 10 bar and 30 °C. As summarized in this table, the $O_2$, $N_2$, $CO_2$, and $CH_4$ permeability will increase with an increasing percentage of carbon nanotubes.

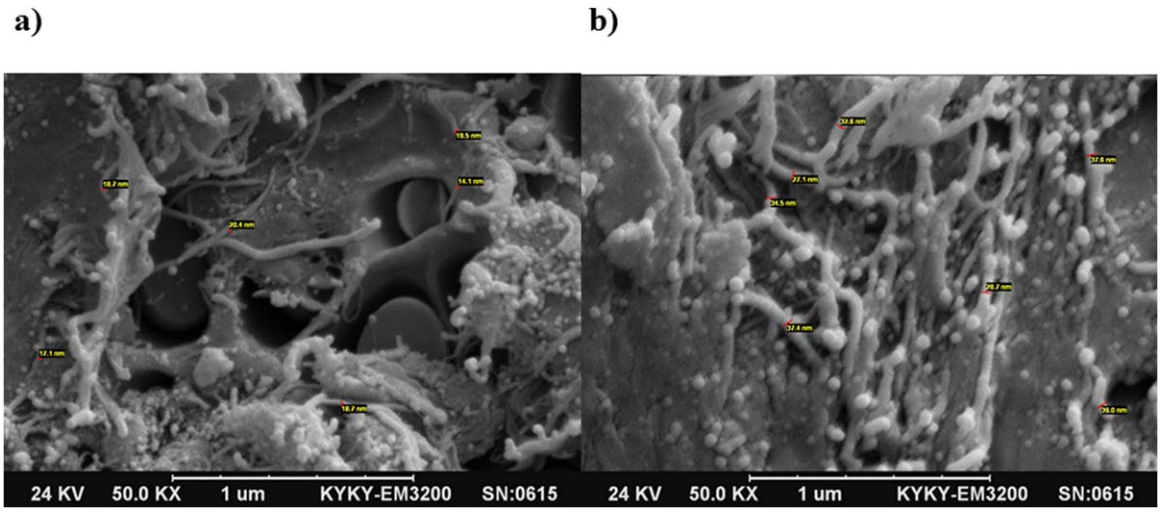


**Figure 5.** Scanning electron microphotographs of (a) nanocomposite membranes with PSF percentage of 50% in Kapton–PSF and 5% of multilayer carbon nanotube and (b) nanocomposite membranes with PSF percentage of 50% in Kapton–PSF and 8% of multilayer carbon nanotube. [Color figure can be viewed in the online issue, which is available at wileyonlinelibrary.com.]

**Table I.** Permeability and Selectivity of Pure Gases through Nanocomposite Kapton–PSF Membranes at Conditions of 10 bar and 30 °C

| Membrane Kapton/PSF (50/50 wt %) | Permeability (Barrer) | | | | Selectivity | | |
|---|---|---|---|---|---|---|---|
| | $CH_4$ | $CO_2$ | $N_2$ | $O_2$ | $CO_2/N_2$ | $CO_2/CH_4$ | $O_2/N_2$ |
| CNT-0 (0 wt % CNT) | 0.2159 | 4.462 | 0.225 | 0.8286 | 19.83 | 20.67 | 3.68 |
| CNT-2.5 (2.5 wt % CNT) | 0.242 | 4.714 | 0.24 | 0.8636 | 19.64 | 19.47 | 3.598 |
| CNT-5 (5 wt % CNT) | 0.27 | 5.146 | 0.262 | 0.9356 | 19.64 | 19.05 | 3.571 |
| CNT-8 (8 wt % CNT) | 0.32 | 5.434 | 0.31 | 1.0075 | 17.53 | 16.98 | 3.25 |

**Table II.** Physical Properties of Various Gases and Equilibrium Isotherm Parameters for Membranes

| Gas | *d* (Å) | Molecular weight | Viscosity, $\eta \times 10^7$ (Pa s) | Condensability (K) |
|---|---|---|---|---|
| $N_2$ | 3.64 | 28.01 | 178 | 195 |
| $CH_4$ | 3.80 | 16.04 | 116 | 107 |
| $CO_2$ | 3.30 | 44.01 | 148 | 71 |
| $O_2$ | 3.46 | 32.1 | 201 | 149 |

This behavior is due to the change of free volume and empty spaces. The presence of nanotubes in a mixed matrix modifies the network chains and changes the free volume. In fact, a suitable space will be provided for gas transport, and the permeability of gases through the membrane will also be increased due to making the carbon nanotube structure and the existence of a capillary in the nanotube. An assessment of the behavior of gas permeability in membranes and nanocomposite membranes demonstrates that the order of gas permeability in a mixed-matrix membrane is as follows:

$$P_{CO_2} > P_{O_2} > P_{N_2} > P_{CH_4}$$

The high permeability of $CO_2$ is due to the higher solution of carbon dioxide in comparison to other gases in a composite membrane. Since $CO_2$ molecules are smaller than the other gases (in this study) from a molecular point of view, this facilitates the influence of this gas in the productivity of a membrane (data from Table II). It is noted that the dominant mechanism of gas transport through polymer membranes is a solution–diffusion mechanism. Regarding this mechanism, polymers act as molecular screens, and gases of smaller size will pass through more quickly. As a whole, they highly influence the phenomenon of gas transport. A comparison of the results of $CH_4$ and $N_2$ permeability leads to a conclusion that the permeability of these gases are similar (Figure 6). It is expected that the permeability values of these gases are different from one another since this matrix has been derived from a blend of glass polymers. This is the result of phase separation in the blended membrane. As mentioned, the two polymers of the case study are not well adapted to each other. This increases the solution of the condensable gas of methane, and it is considered to be a remedy for the lack of its influence in the membrane. Therefore, the permeabilities of these two gases (solution × diffusion) will be very close.

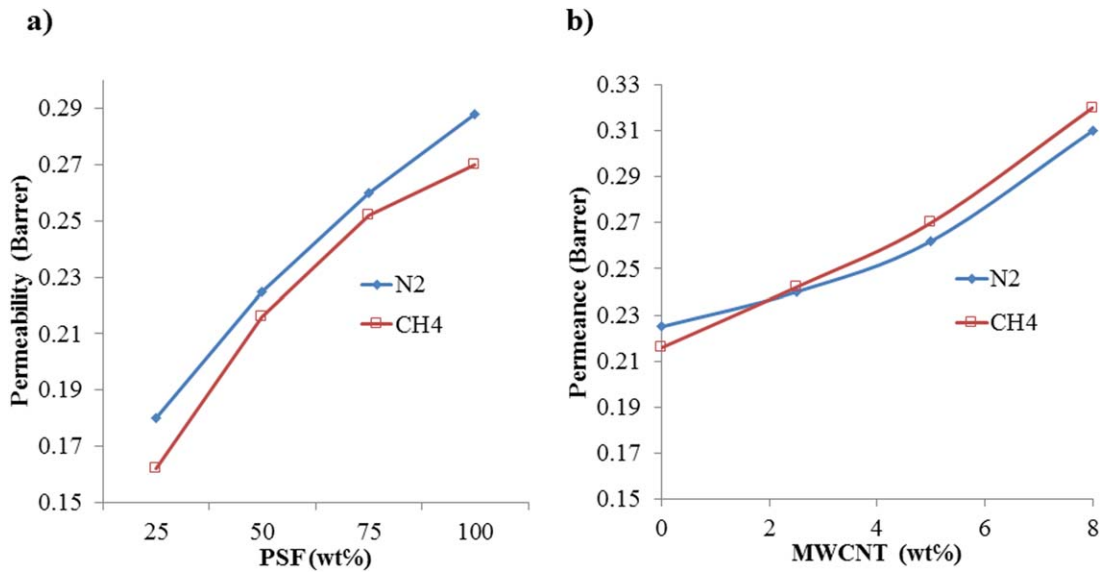


**Figure 6.** Results of nitrogen and methane permeability for composite membranes derived from Kapton–PSF at 10 bar and 30 °C versus (a) various percentages of PSF and (b) various percentages of carbon nanotubes. [Color figure can be viewed in the online issue, which is available at wileyonlinelibrary.com.]

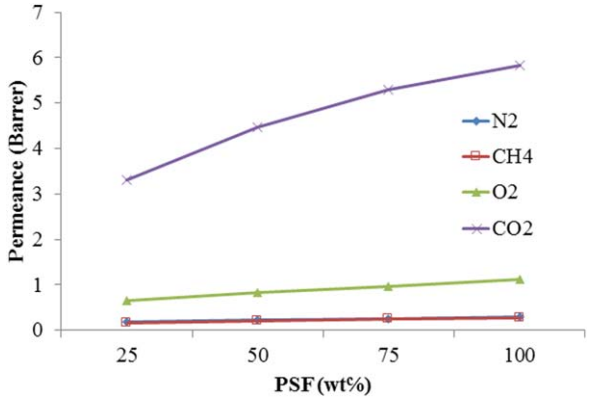


**Figure 7.** Results of pure gas permeability for Kapton–PSF composite membranes at 10 bar and 30 °C. [Color figure can be viewed in the online issue, which is available at wileyonlinelibrary.com.]

The results for gas permeability in nanocomposite membranes reveal that adding nanoparticles increases the $CH_4$ permeability more than the nitrogen permeability, and the order of gas permeability is modified as below:

$$P_{CO2} > P_{O2} > P_{CH4} > P_{N2}$$

It is observed that $CH_4$ with its larger size has more permeability than $N_2$. Contemplation of the molecular specifications of gases determines that $CH_4$ has more condensability than $N_2$. This fact proves that the presence of carbon nanotubes in the structure provides suitable capillaries in the membrane. Since there is a good absorption space on the surface, the gases are absorbed better. As a matter of fact, $CH_4$ is more condensable, and it can be absorbed into the structure. In fact, its permeability is increased. This phenomenon indicates that the presence of carbon nanotubes in the structure will increase the effect of the solution mechanism in gas permeability.

Figure 7 displays the gas permeability of Kapton–PSF blend precursors with various PSF compositions and their corresponding nanocomposite membranes for $N_2$, $CH_4$, $O_2$, and $CO_2$. In contrast, a smaller increase in $CH_4$ and $N_2$ permeability was observed. Tables III represents the gas-transport properties and separation performance of Kapton–PSF/nanocomposite membranes and also the measured gas permeation values for the precursors fabricated from blends of Kapton and PSF. The data in these tables show that adding carbon nanotubes to the structure of the membrane diminishes the ideal selectivity of all gases. Figure 8 illustrates the $O_2/N_2$ and $CO_2/CH_4$ gas pair selectivity of composite membranes derived from Kapton–PSF at 10 bar and 30 °C versus various percentages of PSF and carbon nanotubes.

Increasing the percentage of PSF in the matrix network of membranes enhances the permselectivity of $CO_2/CH_4$. However, a minor improvement was observed in the ideal selectivity of

**Table III.** Permeability and Selectivity of Pure Gases through Nanocomposite/Kapton–PSF Membranes (25/75%) at Conditions of 10 bar and 30 °C

| Membrane (Kapton/PSF) (25/75 wt %) | Permeability (Barrer) | | | | Selectivity | |
|---|---|---|---|---|---|---|
| | $CH_4$ | $CO_2$ | $N_2$ | $O_2$ | $CO_2/CH_4$ | $O_2/N_2$ |
| CNT-0 (0 wt % CNT) | 0.252 | 5.298 | 0.26 | 0.972 | 21.01 | 3.74 |
| CNT-2.5 (2.5 wt % CNT) | 0.261 | 5.432 | 0.259 | 0.989 | 20.81 | 3.82 |
| CNT-5 (5 wt % CNT) | 0.295 | 5.89 | 0.28 | 1.06 | 19.97 | 3.786 |
| CNT-8 (8 wt % CNT) | 0.35 | 6.2 | 0.34 | 1.15 | 17.71 | 3.38 |

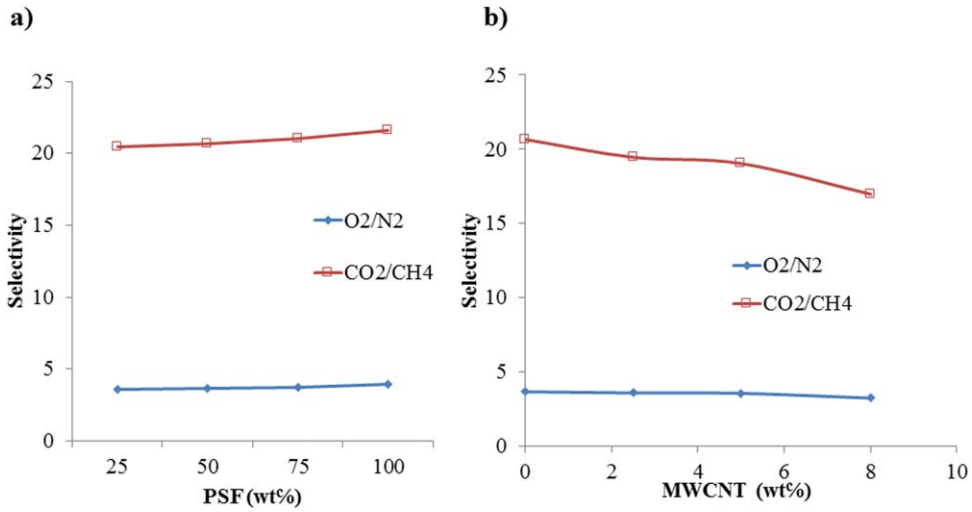


**Figure 8.** Results of $O_2/N_2$ and $CO_2/CH_4$ selectivity of composite membranes derived from Kapton–PSF at 10 bar and 30 °C versus (a) various percentages of PSF and (b) various percentages of carbon nanotubes. [Color figure can be viewed in the online issue, which is available at wileyonlinelibrary.com.]

$O_2/N_2$ for a blended membrane with higher PSF. It is essential to consider that there is only a minor difference in the kinetic diameter ($d$) of oxygen and nitrogen. Figure 8(b) demonstrates the separation performance of Kapton–PSF/nanocomposite membranes for $O_2/N_2$ and $CO_2/CH_4$ separations for various carbon nanotube percentages. The data in this figure clearly specify the impact of carbon nanotubes on $O_2/N_2$ and $CO_2/CH_4$ selectivity. In general, the ideal selectivity of nanocomposite membranes with higher percentages of carbon nanotubes was lower than for other membranes. However, the $O_2/N_2$ selectivity remained constant for all the percentages of carbon nanotubes in composites. As mentioned before, adding carbon nanotubes provides more empty spaces for transporting gas molecules, so the gas permeability is increased as well. Meanwhile, providing such spaces and their existence in the structure of the membrane decreases the screening specifications of the membrane and degrades the selectivity for gases. Finally, it can be generally stated that the increase of the carbon nanotubes in the membrane structure reduces the selectivity of all gases. As pointed out, the addition of carbon nanotubes creates the void spaces for gases to pass through. This will result in increasing permeability. Besides the presence and creation of these spaces in the membrane structure, the gas pair separation will be reduced in the membrane, and the selectivity of gases will be diminished.

## CONCLUSIONS

Advanced nanocomposite membranes were developed by incorporating carbon nanotubes into blended polymers composed of different ratios of Kapton and PSF in their chemical structures. The effect of different percentages of PSF and carbon nanotubes was investigated on the performance for gas-separation applications of the membranes developed here. The percentage of PSF was important in controlling the gas permeability and ideal selectivity of the precursors and the nanocomposite membranes derived from PSF. For the nanocomposite membranes, the trend was as follows: $P_{CO2} > P_{O2} > P_{CH4} > P_{N2}$. Nanocomposite membranes derived from Kapton–PSF with higher percentages of PSF exhibited more remarkable gas permeability than the other blends. It should be considered that a higher PSF content can result in improved permeability but less selectivity, particularly for $CO_2/N_2$, $CO_2/CH_4$, and $O_2/N_2$ separation. Also, membranes derived from PI–PSF (25/75 wt %) exhibited more attractive gas-separation performance than the other blends, in which a higher PSF content could result in improved permeability while enhancing selectivity. The results of the characterization tests indicated that the existence of nanotubes in the polymer structure provides some fibers in the membrane, reflecting a suitable and nanometric distribution of particles in the membrane. The permeability of $CH_4$, $CO_2$, $N_2$, and $O_2$ increased from 0.216, 4.462, 0.225, and 0.829 Barrer (at no loading of CNT and pressure of 10 bar) to 0.32, 5.434, 0.31, and 1.007 Barrer (at 8 wt % of CNT and 10 bar), respectively, with imperceptible changes in gas pair selectivity. The nanocomposite membranes developed in this research can be applied as membranes with effective performance for various gas applications.

## REFERENCES


1. Pirouzfar, V.; Hosseini, S. S.; Omidkhah, M. R.; Moghaddam, A. Z. *Polym. Eng. Sci.* **2014**, *54*, 147.
2. Pirouzfar, V. High Performance Gas Separation Carbon Molecular Sieve Membranes; Lambert, Saarbrücken, Germany ISBN: 978-3-659-19304-0.
3. Petersen, J.; Peinemann, K.-V. *J. Appl. Polym. Sci.* **1997**, *63*, 1557.
4. Armstrong, S. R.; Offord, G. T.; Paul, D. R.; Freeman, B. D.; Hiltner, A.; Baer, E. *J. Appl. Polym. Sci.* **2014**, 131, DOI: 10.1002/app.39765.
5. Mannan, H. A.; Mukhtar, H.; Murugesan, T.; Nasir, R.; Mohshim, D. F.; Mushtaq, A. *Chem. Eng. Technol.* **2013**, *36*, 1838.
6. Saufi, S. M.; Ismail, A. F. *Carbon* **2004**, *42*, 241.
7. Huang, M.-R.; Li, X.-G.; Ji, X.-L.; Qiu, W.; Gu, L.-X. *J. Appl. Polym. Sci.* **2000**, *77*, 2396.
8. Yokwana, K.; Gumbi, N.; Adams, F.; Mhlanga, S.; Nxumalo, E.; Mamba, B. *J. Appl. Polym. Sci.* **2015**, *132*, DOI: 10.1002/app.41835.
9. Shi, B.; Feng, C.; Wu, Y. *J. Appl. Polym. Sci.* **2005**, *95*, 871.
10. Seoane, B.; Coronas, J.; Gascon, I.; Benavides, M. E.; Karvan, O.; Caro, J.; Kapteijna, F.; Gascon, J. *Chem. Soc. Rev.* **2015**, *44*, 2421.
11. Nabian, N.; Ghoreyshi, A. A.; Rahimpour, A.; Shakeri, M.; Korean, J. *Chem. Eng.* **2015**, 32(11), 2204.
12. Baker, R. W. *Ind. Eng. Chem. Res.* **2002**, *41*, 1393.
13. Robeson, L. M. *J. Membr. Sci.* **1991**, *62*, 165.
14. Robeson, L. M. *J. Membr. Sci.* **2008**, *320*, 390.
15. Sun, H.; Ma, C.; Yuan, B.; Wang, T.; Xu, Y.; Xue, Q.; Li, P.; Kong, Y. *Sep. Purif. Technol.* **2014**, *122*, 367.
16. Song, H. J.; Jo, Y. J.; Kim, S.-Y.; Lee, J.; Kim, C. K. *J. Membr. Sci.* **2014**, *466*, 173.
17. Ahn, J.; Chung, W.-J.; Pinnau, I.; Guiver, M. D. *J. Membr. Sci.* **2008**, *314*, 123.
18. Merkel, T. C.; Freeman, B. D.; Spontak, R. J.; He, Z.; Pinnau, I.; Meakin, P.; Hill, A. *J. Science* **2002**, *296*, 19.
19. Kim, S.; Marand, E. *Microporous Mesoporous Mater.* **2008**, *114*, 129.
20. Esfahani, M. R.; Tyler, J. L.; Stretz, H. A.; Wells, M. J. M. *Desalination* **2015**, *372*, 47.
21. Slater, A. G.; Cooper, A. I. *Science* **2015**, *348*, 8075.
22. Li, K. Ceramic Membranes for Separation and Reaction; John Wiley & Sons: **2007**, ISBN: 978-0-470-01440-0.
23. Hsieh, H. P. In Inorganic Membranes for Separation and Reaction; Elsevier: Amsterdam, **1996**; pp 1–13.
24. Burggraaf, A. J.; Keizer, K. In Inorganic Membranes: Synthesis, Characteristics, and Applications; Bhave, R. R., Ed.; Van Nostrand Reinhold: New York, **1991**; pp 10–63.
25. Yampolskii, Y.; Pinnau, I.; Freeman, B. D. Materials Science of Membranes for Gas and Vapor Separation; John Wiley & Sons:Austin, Texas, **2006**; ISBN: 0-470-85345-X.

26. Hinds, B. J.; Chopra, N.; Rantell, T.; Andrews, R.; Gavalas, V.; Bachas, L. G. *Science* **2004**, *303*, 62.
27. Cong, H.; Zhang, J.; Radosz, M.; Shen, Y. *J. Membr. Sci.* **2007**, *294*, 178.
28. Weng, T. H.; Tseng, H. H.; Wey, M. Y. *Int. J. Hydrogen Energy* **2009**, *34*(20), 8707.
29. Aroon, M. A.; Ismail, A. F.; Montazer-Rahmati, M. M.; Matsuura, T. *J. Membr. Sci.* **2010**, *364*, 309.
30. Goh, P. S.; Ng, B. C.; Ismail, A. F.; Sanip, S. M.; Aziz, M.; Kassim, M. A. *Sep. Sci. Technol.* **2011**, *46*, 1250.
31. Ge, L.; Zhu, Z.; Rudolph, V. *Sep. Purif. Technol.* **2011**, *78*, 76.
32. Ge, L.; Zhu, Z.; Li, F.; Liu, S.; Wang, L.; Tang, X.; Rudolph, V. *J. Phys. Chem. C* **2011**, *115*, 6661.
33. Favvas, E. P.; Nitodas, S. F.; Stefopoulos, A.; Stefanopoulos, K. L.; Papageorgiou, S. K.; Mitropoulos, A. *Ch. Sep. Purif. Technol.* **2014**, *122*, 262.
34. Caro, J.; M, Noack P. Kölsch, R. Schäfer. *Microporous Mesoporous Mater.* **2000**, *38*, 3.
35. Pirouzfar, V.; Hosseini, S. S.; Omidkhah, M. R.; Moghaddam, A. Z. *J. Ind. Eng. Chem.* **2014**, *20*, 1061.
36. Hosseini, S. S.; Omidkhah, M. R.; Moghaddam, A. Z.; Pirouzfar, V. *Sep. Purif. Technol.* **2014**, *122*, 278.
37. Fuertes, A. B.; Centeno, T. A. *Carbon* **1999**, *37*, 679.
38. Centeno, T. A.; Fuertes, A. B. *Sep. Purif. Technol.* **2001**, *25*, 379.
39. Arjmandi, M.; Pakizeh, M.; Pirouzram, O. *Korean J. Chem. Eng.* **2015**, *32*, 1178.
40. Zarrinkhameh, M.; Zendehnam, A.; Hosseini, S. M. *Korean J. Chem. Eng.* **2014**, *31*, 1187.
41. Zendehnam, A.; Rabieyan, M.; Hosseini, S. M.; Mokhtari, S. *Korean J. Chem. Eng.* **2015**, *32*, 501.
42. Sieffert, D.; Staudt, C. *Sep. Purif. Technol.* **2011**, *77*, 99.
43. Tofighy, M. A.; Mohammadi, T. *Korean J. Chem. Eng.* **2014**, *32*, 292.
44. Favvas, E. P.; Stefanopoulos, K. L.; Nolan, J. W.; Papageorgiou, S. K.; Mitropoulos, A. Ch.; Lairez, D. *Sep. Purif. Technol.* **2014**, *132*, 336.
45. Ge, L.; Zhu, Z.; Rudolph, V. *Sep. Purif. Technol.* **2011**, *78*, 76.
46. Favvas, E. P.; Nitodas, S. F.; Stefopoulos, A.; Stefanopoulos, K. L.; Papageorgiou, S. K.; Mitropoulos, A. *Ch. Sep. Purif. Technol.* **2014**, *122*, 262.
47. Song, H. J.; Jo, Y. J.; Kim, S.-Y.; Lee, J.; Kim, C. K. *J. Membr. Sci.* **2014**, *466*, 173.
48. Rezakazemi, M.; Amooghin, A. E.; Montazer-Rahmati, M. M.; Ismail, A. F.; Matsuura, T. *Prog. Polym. Sci.* **2014**, *39*, 817.
49. Aroon, M. A.; Ismail, A. F.; Matsuura, T.; Montazer-Rahmati, M. M. *Sep. Purif. Technol.* **2010**, *75*, 229.
50. Mollahosseini, A.; Rahimpour, A.; Jahamshahi, M.; Peyravi, M.; Khavarpour, M. *Desalination* **2012**, *306*, 41.
51. Kim, S.; Marand, E. *Microporous Mesoporous Mater.* **2008**, *114*, 129.
52. Goh, P. S.; Ismail, A. F.; Sanip, S. M.; Ng, B. C.; Aziz, M. *Sep. Purif. Technol.* **2011**, *81*, 243.
53. Laot, C. M.; Marand, E.; Schmittmann, B.; Zia, R. K. P.; Macromolecules.10/2003; 36(23). DOI: 10.1021/ma021720o.
54. Suda, H.; Haraya, K. *J. Phys. Chem. B* **1997**, *101*, 3988.
55. Fuertes, A. B.; Nevskaia, D. M.; Centeno, T. A. *Microporous Mesoporous Mater.* **1999**, *33*, 115.
56. Peterson, J.; Matsuda, M.; Haraya, K. *J. Membr. Sci.* **1997** *131*, 85.
57. Marand, E.; Kim, S.; Pechar, T. W. *Desalination* **2006**, *192*, 330.
58. Ansaloni, L.; Zhao, Y.; Jung, B. T.; Ramasubramanian, K.; Baschetti, M. G.; Ho, W. S. W. *J. Membr. Sci.* **2015**, *490*, 18.
59. Zhao, D.; Ren, J.; Li, H.; Li, X.; Deng, M. *J. Membr. Sci.* **2014**, *467*, 41.
60. Baroña, G. N. B.; Choi, M.; Jung, B. *J. Colloid Interface Sci.* **2012**, *386*, 189.
61. Kiadehi, A. D.; Rahimpour, A.; Jahanshahi, M.; Ghoreyshi, A. A. *J. Ind. Eng. Chem.* **2015**, *22*, 199.
62. Grosso, V.; Vuono, D.; Bahattab, M. A.; Di Profio, G.; Curcio, E.; Al-Jilil, S. A.; Alsubaie, F.; Alfife, M.; Nagy, J. B.; Drioli, E.; Fontananova, E. *Sep. Purif. Technol.* **2014**, *132*, 684.
63. Pal, G.; Kumar, S. *Prog. Aerospace Sci.* **2016**, *80*, 33.
64. George, G.; Bhoria, N.; AlHallaq, S.; Abdala, A.; Mittal, V. *Sep. Purif. Technol.* **2016**, *158*, 333.